

NANO EXPRESS

Open Access



One-step electrospinning route of SrTiO₃-modified Rutile TiO₂ nanofibers and its photocatalytic properties

Weijie Zhao^{1,2}, Jing Zhang², Jiaqi Pan¹, Jianfeng Qiu¹, Jiantao Niu¹ and Chaorong Li^{1*}

Abstract

The SrTiO₃ modified rutile TiO₂ composite nanofibers were synthesized by a simple electrospinning technique. The result of XRD, SEM and TEM indicate that the SrTiO₃/TiO₂ heterojunction has been prepared successfully. Compared with the TiO₂ and SrTiO₃, the photocatalytic activity of the SrTiO₃/TiO₂ (rutile) for the degradation of methyl orange exhibits an obvious enhancement under UV illumination, which is almost 2 times than that of bare TiO₂ (rutile) nanofiber. Further, the high crystallinity and photon-generated carrier separation of the SrTiO₃/TiO₂ heterojunction are considered as the main reason for this enhancement.

Keywords: Electrospinning, Heterojunction, Photocatalyst, Recycling

Background

As a prototypical semiconductor with environment friendly and high photoelectric property, Titanium oxide (TiO₂) is widely used in optics, solar cells, sensors etc. [1–4], and also considered as a most promising photocatalyst in wastewater treatments [5], due to its low cost, highly physical-chemical stability and nontoxicity. As previous literature reported, though the anatase TiO₂ exhibit better photocatalysis than the Rutile TiO₂, but the band gap of anatase TiO₂ (3.2 eV) is wider than the rutile TiO₂ (3.0 eV), which may restrict the luminous energy utilization ratio in photocatalytic application. What's more, compare with the metastable anatase TiO₂, the rutile TiO₂ exhibit more highly physical-chemical stability, which is beneficial for cyclic utilization in pollution treatment. With these unique advantages, how to improve the photocatalytic efficiency of the rutile TiO₂ would be a significant issue. As known, the photocatalysis mainly depend on specific surface area or mobility and lifetime of photon-generated carriers, so lots of work have been reported. For specific surface area, lots of excellent morphology have been prepared, such as nanosheets [6], nanobelts [7], nanorods [8], nanofibers [9], and microflowers [10], all of them shows a

inspiring results [11–14]. On the other hand, the surface noble metal modified or preparation of heterostructure are considered as useful ways to adjust the band structure for improving the mobility and lifetime of photon-generated carriers. However, compared with the high cost of the noble metal modified, the heterostructure is deemed as a efficient-low cost way. Lots of relevant researches have been reported, such as ZnO/TiO₂ [15–17], CdS/ZnO [18–20], CeO₂/graphene etc [21]. Among those semiconductors, the strontium titanate (SrTiO₃) has caught researchers attention due to the thermal stability and resistance to photocorrosion [22], and has been extensively applied in H₂ generation [23], removal of NO [24], water splitting [25], and photocatalyst decomposition of dye [26–28]. In particular, as heterostructures composite photocatalyst attracted more attention, such as, Core-shell SrTiO₃/TiO₂ and heterostructures SrTiO₃/TiO₂ had showed much higher photocatalytic activity than the pure TiO₂, which is attributed to heterostructures promote the separation of photogenerated carriers [29, 30]. So the SrTiO₃ is considered as a good candidate for coupling with the anatase phase of TiO₂ for adjusting the band structure to enhance its photocatalytic activity. However, there are rare reports about the SrTiO₃-modified rutile TiO₂ composites nanofibers for the degradation of dye pollutants because of the cumbersome process, so how to simplify the preparation of SrTiO₃/TiO₂ nano-heterojunction would be an important

* Correspondence: crli@zstu.edu.cn

¹Department of Physics and Key Laboratory of ATMMT Ministry of Education, Zhejiang Sci-Tech University, Hangzhou 310018, People's Republic of China
Full list of author information is available at the end of the article

issue for its practical application. As known, the electrospinning is a convenient and efficient method to prepared nanomaterials, which could easily prepare the precursor into nanofibers at the preclusion and then form to series of nanostructure in subsequent annealing, which has been reported in lots literatures [31–36].

In the present study, we report on a simple one-step synthesis of SrTiO₃ modified rutile TiO₂ nano-heterojunction with high photocatalysis via the electrospinning. Then the mechanism of the photocatalytic enhancement of the heterojunction has been studied.

Methods

Materials

Analytical grade acetic acid, N,N-Dimethylformamide (DMF, Aladdin, 99.5%), Tetra butyl titanate (TBT, Aladdin, 99.0%), Strontium acetate (Aladdin, 99.97%), Polyvinylpyrrolidone (PVP, M_w = 1,300,000) were obtained from Shanghai Macklin Biochemical Co. Ltd.

Preparation of SrTiO₃/TiO₂ (rutile) Composite Nanofiber

SrTiO₃/TiO₂ (rutile) composite nanofibers was synthesized by directly electrospinning with subsequent calcinations method are shown in Fig. 1. Firstly, the precursor solution was prepared by dissolving 2.2 g PVP into 8 mL DMF and 2 mL acetic acid. After stirring 8 h, 2 g of TBT was added to the precursor solution for 4 h with a magnetic stirrer. Further, a certain amount of strontium acetate was slowly added into above mixture and stirred until the solution is transparent. The prepared sol-gels were loaded in glass syringe, fitted with a 0.5 mm diameter stainless steel needle and clamped in syringe pump (0.6 ml/h, KDS-200, KD Scientific, United States). This needle is connected to the positive electrode of 15 kV (Model: ES40P-10 W, Gamma HighVoltage, United States). A distance of 15 cm was maintained between the needle tip and the grounded aluminum foil

collector. During electrospinning process, the humidity was maintained at <40%, and the ambient temperature was 20 °C. Non-woven nanofiber webs were consequently obtained at the collector and left in an oven at 80 °C drying 6 h. The electrospun nanofibers were calcined in the air at 700 °C (5 °C / min heating) for 1 h to obtain the different ration of SrTiO₃/TiO₂(rutile) nano-heterojunction. What's more, a bare TiO₂(rutile) nanofibers and SrTiO₃ nanofibers were prepared for contrast. The different ration of SrTiO₃ in SrTiO₃/TiO₂ (rutile) nano-heterojunction was 1 wt%, 3 wt%, 5 wt% and 10 wt%, and marked as ST-1, ST-3, ST-5, ST-10, respectively.

Characterization

The surface morphology of the as-prepared samples was investigated by the Field-emission scanning electron microscope (FESEM, Hitachi S-4800) equipped with Energy-dispersive X-ray spectroscopy (EDS), and the microstructure of the as-prepared samples was observed by a transmission electron microscope (TEM, JEM-2100, 200 kV); Crystal structures of the as-prepared samples were characterized by Bruker/D8-advance with Cu K α radiation ($\lambda = 1.518 \text{ \AA}$) at the scanning rate of 0.2 sec/step in the range of 10–80°. The absorption spectrum of the as-prepared samples were recorded using by a UV–visibles petrophotometer (U-3900Hitachi).

Measurement of photocatalytic activity

A 50 mL methyl orange (MO) solution with an initial concentration of 15 mg/L in the presence of sample(30 mg) was filled in a quartz reactor. The light source was provided by a UV – C mercury lamp (Philips Holland, 25 W). Prior to irradiation, the solution was continuously kept in dark for 30 min to reach an adsorption–desorption equilibrium between organic substrates and the photocatalysts. At given intervals (t = 10 min) of irradiation, the samples of the reaction solution were

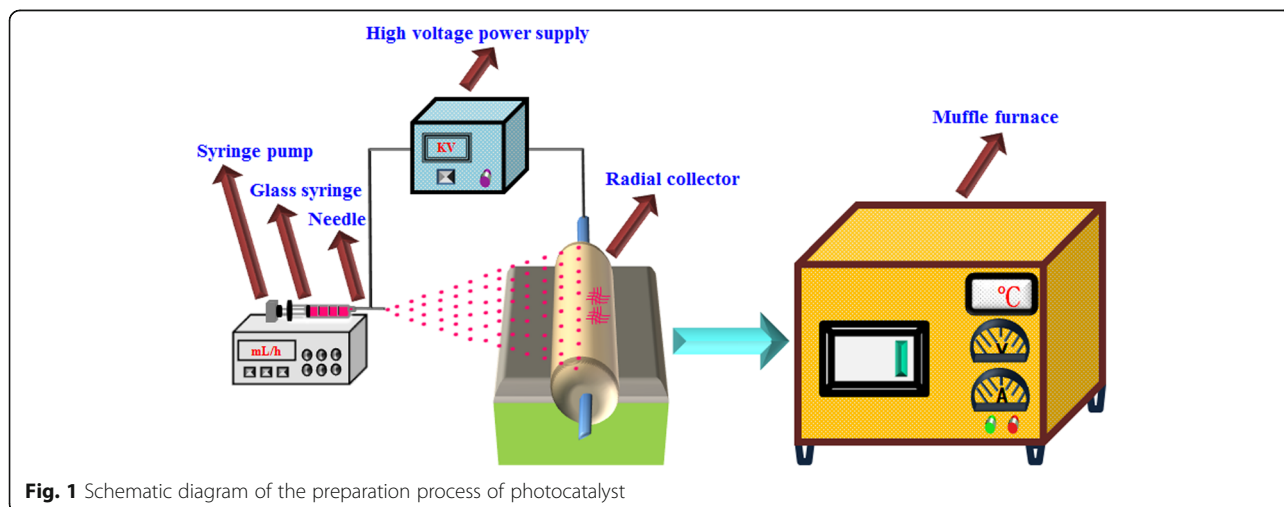


Fig. 1 Schematic diagram of the preparation process of photocatalyst

taken out and analyzed. The concentrations of the remnant dye were measured with a spectrophotometer at $\lambda = 464$ nm.

Results and discussion

Figure 2 displayed the XRD patterns of rutile TiO_2 , SrTiO_3 and the different concentration of $\text{SrTiO}_3/\text{TiO}_2$ (rutile) nano-heterojunction. It is obvious that the diffraction peaks at $2\theta = 27.5, 36.1, 41.3$ and 54.4° can be indexed to the (110), (101), (111), (211) crystal planes of rutile TiO_2 (JCPDS78-1510). The peaks at $32.4, 40.0, 46.5,$ and 57.8° are attributed to the (110), (111), (200), and (211) crystal planes of Cubic SrTiO_3 (JCPDS 84-0443). The result indicates that the $\text{SrTiO}_3/\text{TiO}_2$ (rutile) composite nanofibers with higher crystallinity are successfully prepared under 700°C sintering (Fig. 2), which may be beneficial to promote the photon-generated carrier transporting to increasing the photocatalysis.

The surface morphology of the as-spun ST-3 measured by FESEM was shown in Fig. 3(a)-(d). The unsintered ST-3 preliminary composite nanofiber was illustrated in Fig. 3 (a). As shown, the surface of obtained nanofibers with diameter approximately 300 nm is smooth and continuous. Since TBT could be rapidly hydrolyzed by moisture in the air, continuous networks of TiO_2 sols were formed in the nanofibers once they had been ejected from the needle tip [37]. As presented in Fig. 3(b), after sintering at 700°C , the diameter of nanofibers decreased to about 200 nm and the fibers are still continuous. It's interesting that the fiber after sintering, the nanofibers became slender and

rough, which could generate much more specific surface area to increase the photocatalysis.

The TEM images provided further insight about the crystal structure of ST-3 composite nanofibers. Figure 4a shows a typical TEM image for ST-3, which is corresponded to the SEM. HRTEM was employed to further illuminate the crystal structures of rutile ST-3 composite nanofibers. As shown in Fig. 4b, the high magnification HRTEM image reveals clearly indicates two distinctive lattice of 0.324 nm and 0.275 nm respectively, which correspond to the (110) plane of rutile TiO_2 and the (110) plane of SrTiO_3 . This result also indicates that the nano-heterojunction have formed in the $\text{SrTiO}_3/\text{TiO}_2$ (rutile) composite nanofibers (Fig. 4b), which would be beneficial to separate photogenerated electrons-holes pairs.

The selected area electron diffraction (SAED) as shown in Fig. 4c, which indicates that the nano-heterojunction owns a high crystallinity. The FESEM EDX in Fig. 4d further confirms that ST-3 heteroarchitectures contain the Ti, Sr, O elements and corresponds to the XRD.

MO was used as a model dye pollutant to survey the photocatalytic activity of bare TiO_2 (rutile), bare SrTiO_3 and different $\text{SrTiO}_3/\text{TiO}_2$ (rutile) nanocomposites, and the results were shown in Fig. 5. After 40 min of irradiation, the rutile ST-1, ST-3, ST-5, ST-10, bare TiO_2 (rutile) and bare SrTiO_3 nanofibers had degraded ca. 62%, 93%, 79%, 43%, 47% and 44% of the initial MO dye, respectively (Fig. 5b). It's interesting that, with the increasing concentration of the SrTiO_3 , the photocatalytic activity of $\text{SrTiO}_3/\text{TiO}_2$ (rutile) composite nanofibers exhibit an obviously enhancement, which indicates that the presence of

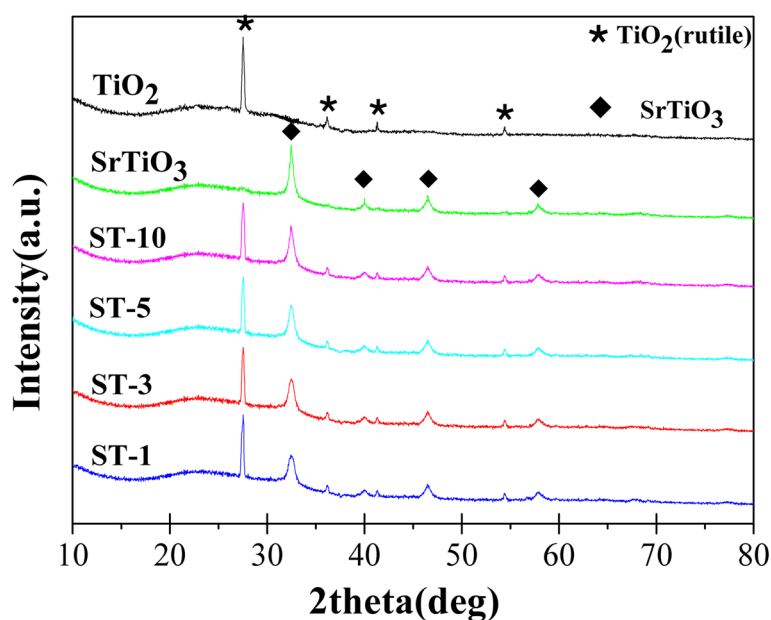


Fig. 2 XRD patterns of the bare TiO_2 (Rutile), bare SrTiO_3 , ST-10, ST-5, ST-3 and ST-1

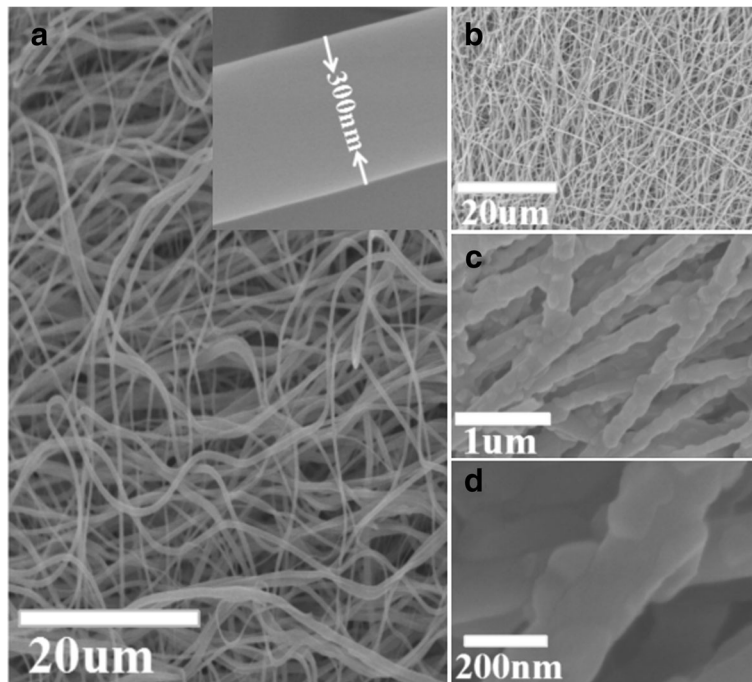


Fig. 3 FESEM image of ST-3. **a** as-prepared ST-3, *inset*: High magnification SEM (unsintered), **(b)-(d)** ST-3 (sintered)

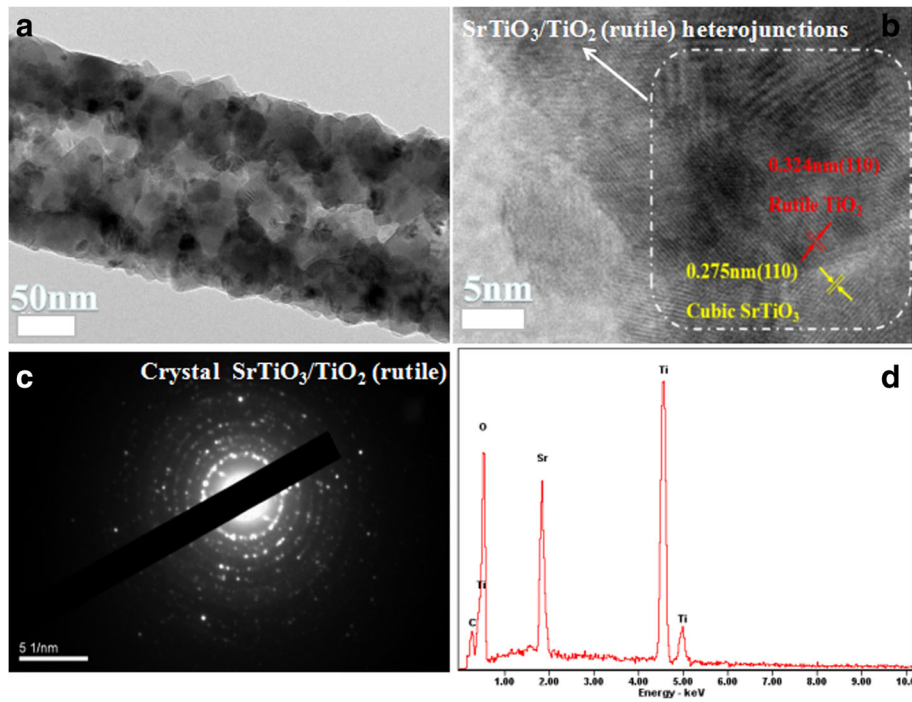
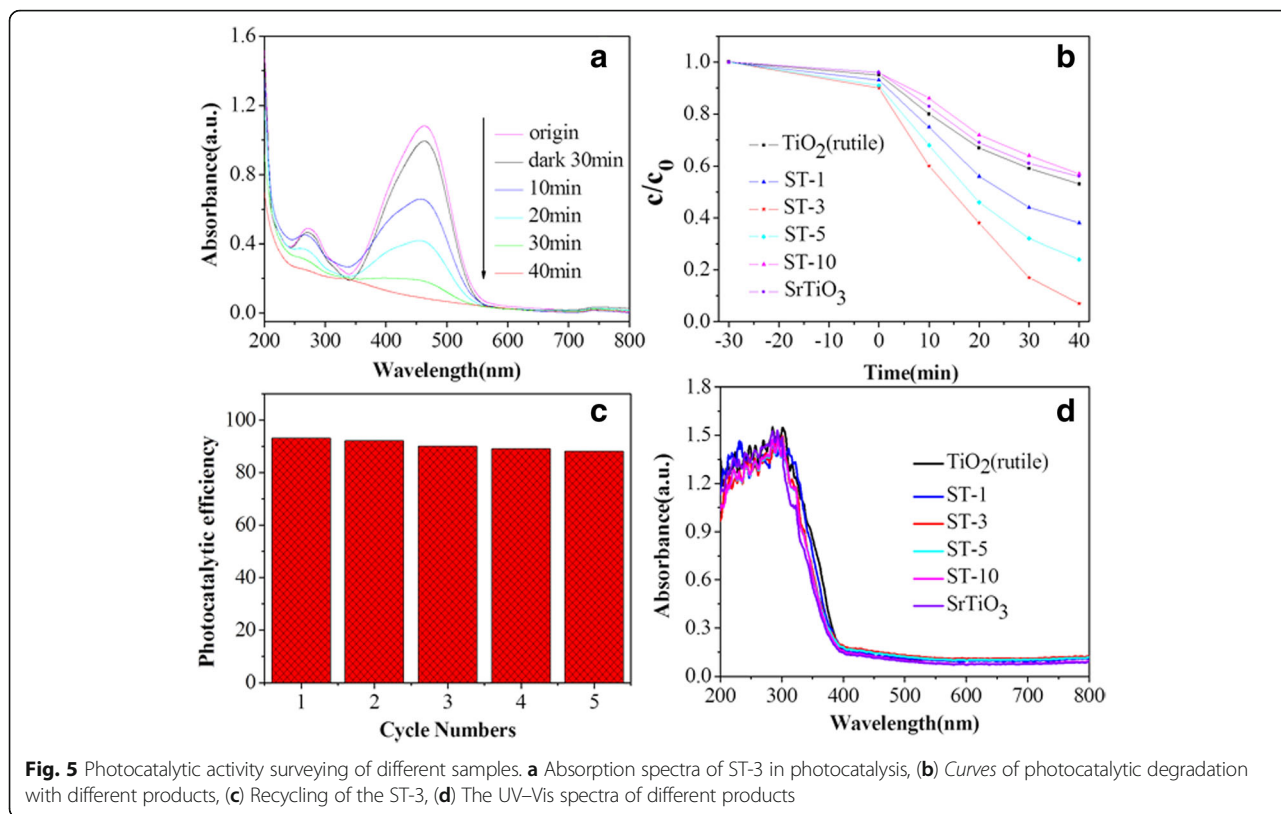


Fig. 4 TEM image and EDS spectrum of ST-3. **a** TEM image of ST-3, **(b)** HRTEM of the delineated area of the rutile TiO_2 and SrTiO_3 , **(c)** SAED of ST-3, **(d)** EDS of ST-3

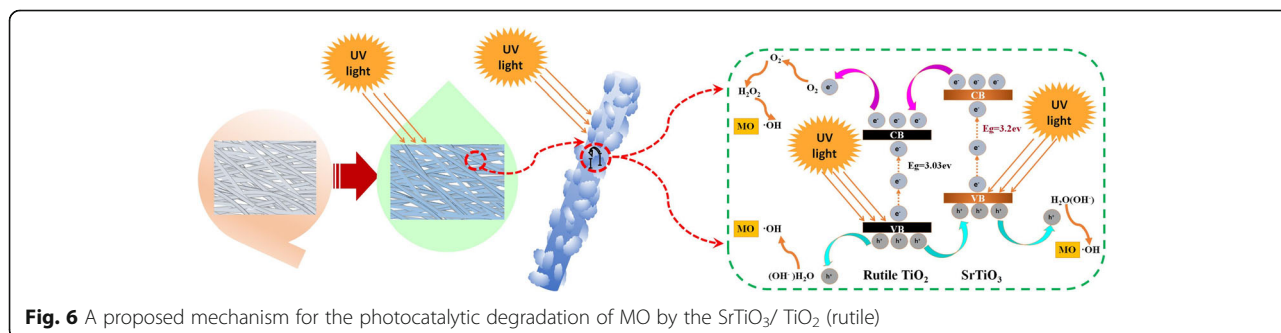


the heterostructure in the composite photocatalyst is beneficial to the photocatalysis. What's more, as shows in the Fig. 5b, when there is excess SrTiO₃, the composites may exhibit a decreasing photocatalytic activity, which could be ascribed to that the photocatalysis of the SrTiO₃ is much weaker than the TiO₂, so suitable SrTiO₃ could form the heterojunction to improve the photocatalysis efficiently but the excess SrTiO₃ may lead an obvious decreasing.

In order to be convenient for long-term photocatalytic use in the treatment of dye wastewater, the cycling stability is one of the most important factor, and was shown in Fig. 5c. As shown in Fig. 5c, after 5 cycles, there is negligible loss of MO photodegradation, which could be ascribed to the lost of photocatalyst in centrifugal

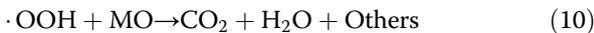
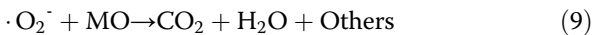
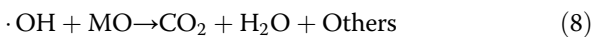
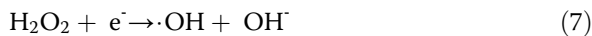
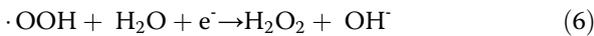
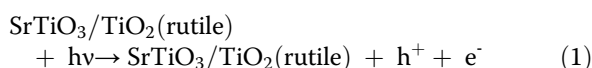
process and further illustrate that the ST-3 composite photocatalysts possess highly stability and cyclicity.

As the excellent photocatalysis, the possible mechanism for the enhanced photocatalytic activity of the SrTiO₃/TiO₂ (rutile) composite nanofibers is very important for its further modified. As shown in Fig. 5d, the absorption of the different samples changes little, it means that the photocatalytic activity is independent with the absorption, which could be attributed to the unique nano-heterojunction. The possible mechanism is represented as follows: When UV light irradiate on surface of the composite nanofibers, both the SrTiO₃ and the rutile TiO₂ could generate holes (h⁺) and electrons (e⁻) as shown in (1). Then the generated electrons are immigrated from the valence band (VB) of SrTiO₃ to



conduction bands (CB) of SrTiO₃, and further transplanted into the conduction band (CB) of rutile TiO₂. On the other hand, the holes are transferred to VB of SrTiO₃ from rutile TiO₂, which could promote the charge separation efficiently to increase the lifetime of the charge carriers and enhance the efficiency of the interfacial charge transferred to enhance the photocatalytic activity of the SrTiO₃/TiO₂(rutile) heterostructure (Fig. 6).

Meanwhile, a probable formula of photocatalytic oxidation of methyl orange was provided as follow:



Therefore, the SrTiO₃/TiO₂ (rutile) composite nanofibers could be considered as an economical and continuous photocatalyst in future application.

Conclusions

In summary, we have prepared the SrTiO₃/TiO₂ (rutile) composite nanofibers via a simple route of electrospinning and displayed its excellent ability to degrade methyl orange, which could be mainly ascribed to the remarkable heterojunction and the high crystallinity. What's more, the novel 3D structure could increase the specific surface area efficiently, which is also an important reason for the photocatalysis. Thus excellent photocatalyst could afford a new sight for design of the future catalyst.

Acknowledgments

This work was supported by Zhejiang Provincial Natural Science Foundation of China (No. LY17E020001, LQ17F040004 and LY15E030011), Natural Science Foundation of China (No. 51672249, 51603187 and 91122022), Taizhou science and technology project of China (1601KY73).

Authors' contributions

WJZ performed the all sample preparation steps and drafted the manuscript. JZ participated in the design of the study. JQP carried out the analysis. JFQ and JTN participated in the measurements. CRL supervised the entire research and polished the manuscript. All the authors have read and approved the final manuscript.

Competing interests

The authors declare that they have no competing interests.

Publisher's Note

Springer Nature remains neutral with regard to jurisdictional claims in published maps and institutional affiliations.

Author details

¹Department of Physics and Key Laboratory of ATMMT Ministry of Education, Zhejiang Sci-Tech University, Hangzhou 310018, People's Republic of China.

²School of Medical and Pharmaceutical Engineering, Taizhou Vocational & Technical College, Taizhou 318000, People's Republic of China.

Received: 13 April 2017 Accepted: 8 May 2017

Published online: 25 May 2017

References

- Nafisah S, Saad SKM, Umar AA, Plucinski K, Lis M, Maciaga A, Miedzinski R (2015) Laser stimulated nonlinear optics of Ag nanoparticle-loaded porous TiO₂ microtablet. *Appl Opt* 45:263–271
- Ma QL, Cui YQ, Deng XY, Cheng XW, Cheng QF, Li B (2017) Controllable Fabrication of TiO₂ Nanobelts/Nanotubes Photoelectrode for Dye Sensitized Solar Cells. *J Nanosci Nanotechnol* 17:2072–2078
- Mishra AK, Huang LP (2015) TiO₂-Decorated Graphite Nanoplatelet Nanocomposites for High-Temperature Sensor Applications. *Small* 11:361–366
- Zhao WJ, Zhang ZC, Zhang J, Wu HG, Xi LM, Ruan CH (2016) Synthesis of Ag/TiO₂/graphene and its photocatalytic properties under visible light. *Mater Lett* 171:182–186
- Zhou SM, Ma DK, Cai P, Chen W, Huang SM (2014) TiO₂/Bi₂(BDC)₃/BiOCl nanoparticles decorated ultrathin nanosheets with excellent photocatalytic reaction activity and selectivity. *Mater Res Bull* 60:64–71
- Zhao DD, Yu YL, Gao DZ, Cao YA (2015) Properties and Photocatalytic Activity of Rutile TiO₂ Nanosheets. *J Inorg Mater* 31:1–6
- Pang LX, Wang XY, Tang XD (2015) Enhanced photocatalytic performance of porous TiO₂ nanobelts with phase junctions. *Solid State Sci* 39:29–33
- Sun MX, Fang YL, Wang Y, Sun SF, He J, Yan Z (2015) Synthesis of Cu₂O/graphene/rutile TiO₂ nanorod ternary composites with enhanced photocatalytic activity. *J Alloy Compd* 650:520–527
- Jung HJ, Kim YL, Jang H, Choia MY, Kimb MH (2016) Pulse laser irradiation of electrospun TiO₂ nanofibers for the crystalline phase control and enhanced photocatalytic activity. *Mater Lett* 181:59–62
- Nair RV, Jijith M, Gummalur VS, Vijayan C (2016) A novel and efficient surfactant-free synthesis of Rutile TiO₂ microflowers with enhanced photocatalytic activity. *Opt Mater* 55:38–43
- Lai LL, Wen W, Wu JM (2016) Ni-doped rutile TiO₂ nanoflowers: low-temperature solution synthesis and enhanced photocatalytic efficiency. *RSC Adv* 6:25511–25518
- Sheikh FA, Appiah-Ntiamoah R, Zargar MA, Chandradass J, Chung WJ, Kim H (2016) Photocatalytic properties of Fe₂O₃-modified rutile TiO₂ nanofibers formed by electrospinning technique. *Mater Chem Phys* 172:62–68
- Lavanya T, Dutta M, Satheesh K (2016) Graphene wrapped porous tubular rutile TiO₂ nanofibers with superior interfacial contact for highly efficient photocatalytic performance for water treatment. *Sep Purif Technol* 168:284–293
- Lu YY, Zhang YY, Zhang J, Shi Y, Li Z, Feng ZC, Li C (2016) In situ loading of CuS nanoflowers on rutile TiO₂ surface and their improved photocatalytic performance. *Appl Surf Sci* 370:312–319
- Kwiatkowski M, Chassagnon R, Heintz O, Geoffroy N, Skompska M, Bezverkhyy I (2017) Improvement of photocatalytic and photoelectrochemical activity of ZnO/TiO₂ core/shell system through additional calcination: Insight into the mechanism. *Appl Catal B: Environ* 204:200–208
- Zalfani M, Schueren B, Mahdouani M, Bourguiga R, Yu WB, Wu M, Deparis O, Li Y, Su BL (2016) ZnO quantum dots decorated 3DOM TiO₂ nanocomposites: Symbiosis of quantum size effects and photonic structure for highly enhanced photocatalytic degradation of organic pollutants. *Appl Catal B: Environ* 199:187–198
- Gondal MA, Ilyas AM, Baig U (2016) Pulsed laser ablation in liquid synthesis of ZnO/TiO₂ nanocomposite catalyst with enhanced photovoltaic and photocatalytic performance. *Ceram Int* 42:13151–13160

18. Dumbrava A, Berger D, Prodan G, Moscalu F (2016) Functionalized ZnO/CdS Composites: Synthesis, Characterization and Photocatalytic Applications. *Chalcogenide Lett* 13:105–115
19. Ge SS, Zhang QX, Wang XT, Qian S, Bao LW, Rui D, Liu QY (2016) Bacteria-Directed Construction of ZnO/CdS Hollow Rods and Their Enhanced Photocatalytic Activity. *J Nanosci Nanotechnol* 16:4929–4935
20. Huo PW, Zhou MJ, Tang YF, Liu XL, Ma CC, Yu LB, Yan YS (2016) Incorporation of N-ZnO/CdS/Graphene oxide composite photocatalyst for enhanced photocatalytic activity under visible light. *J Alloy Compd* 670: 198–209
21. Jiang LH, Yao MG, Liu B, Li QJ, Liu R, Lv H, Lu SC, Gong C, Zou B, Cui T, Liu BB (2012) Controlled Synthesis of CeO₂/Graphene Nanocomposites with Highly Enhanced Optical and Catalytic Properties. *J Phys Chem C* 116: 11741–11745
22. Ohno T, Tsubota T, Nakamura Y, Sayama K (2005) Preparation of S, C cation-codoped SrTiO₃ and its photocatalytic activity under visible light. *Appl Catal A Gen* 288:74–79
23. Cho YJ, Moon GH, Kanazawa T, Maeda K, Choi W (2016) Selective dual-purpose photocatalysis for simultaneous H₂ evolution and mineralization of organic compounds enabled by a Cr₂O₃ barrier layer coated on Rh/SrTiO₃. *Chem Commun* 52:9636–9639
24. Li HH, Yin S, Wang YH, Sekino T, Lee SW, Sato T (2013) Roles of Cr³⁺ doping and oxygen vacancies in SrTiO₃ photocatalysts with high visible light activity for NO removal. *J Catal* 297:65–69
25. Chen W, Liu H, Li XY, Liu S, Gao L, Mao LQ, Fan ZY, Shangguan WF, Fang WJ, Liu YS (2016) Polymerizable complex synthesis of SrTiO₃:(Cr/Ta) photocatalysts to improve photocatalytic water splitting activity under visible light. *Appl Catal B: Environ* 192:145–151
26. Jing PP, Lan W, Su Q, Xie EQ (2015) High photocatalytic activity of V-doped SrTiO₃ porous nanofibers produced from a combined electrospinning and thermal diffusion process. *Beilstein J Nanotechnol* 6:1281–1286
27. Jing PP, Du JL, Wang JB, Lan W, Pan LN, Li JN, Wei JW, Cao DR, Zhang XL, Zhao CB, Liu QF (2015) Hierarchical SrTiO₃/NiFe₂O₄ composite nanostructures with excellent light response and magnetic performance synthesized toward enhanced photocatalytic activity. *Nanoscale* 7:14738–14746
28. Xian T, Yang H, Di LJ, Ma JY, Zhang HM, Dai JF (2014) Photocatalytic reduction synthesis of SrTiO₃-graphene nanocomposites and their enhanced photocatalytic activity. *Nanoscale Res Lett* 9:327–335
29. Zhao W, Liu NQ, Wang HX, Mao LH (2017) Sacrificial template synthesis of core-shell SrTiO₃/TiO₂ heterostructured microspheres photocatalyst. *Ceram Int* 43:4807–4813
30. Cao TP, Li YJ, Wang CH, Shao CL, Liu YC (2011) A Facile in Situ Hydrothermal Method to SrTiO₃/TiO₂ Nanofiber Heterostructures with High Photocatalytic Activity. *Langmuir* 27:2946–2952
31. Sedghia R, Moazzamib HR, Davarania SSH, Nabida MR, Keshtkar AR (2017) A one step electrospinning process for the preparation of polyaniline modified TiO₂/polyacrylonitrile nanocomposite with enhanced photocatalytic activity. *J Alloy Compd* 695:1073–1079
32. Tian FY, Hou DF, Hu FC, Xie K, Qiao XQ, Li DS (2017) Porous TiO₂ nanofibers decorated CdS nanoparticles by SILAR method for enhanced visible-light-driven photocatalytic activity. *Appl Surf Sci* 391:295–302
33. Wang XQ, Dou LY, Yang L, Yu JY, Ding B (2017) Hierarchical structured MnO₂@SiO₂ nanofibrous membranes with superb flexibility and enhanced catalytic performance. *J Hazard Mater* 324:203–212
34. Xu TF, Ni DJ, Chen X, Wu F, Ge PF, Lu WY, Hu HG, Zhu ZX, Chen WX (2016) Self-floating graphitic carbon nitride/zinc phthalocyanine nanofibers for photocatalytic degradation of contaminants. *J Hazard Mater* 317:17–26
35. Pant B, Pant HR, Park M (2014) Electrospun CdS-TiO₂ doped carbon nanofibers for visible-light-induced photocatalytic hydrolysis of ammonia borane. *Catal Commun* 50:63–68
36. Hou DF, Hu XL, Ho WK, Hu P, Huang YH (2015) Facile fabrication of porous Cr-doped SrTiO₃ nanotubes by electrospinning and their enhanced visible-light-driven photocatalytic properties. *J Mater Chem A* 3:3935–3943
37. Zhang XC, Zhang SY, You Y, Li YL (2012) Effect of the Steam Activation Thermal Treatment on the Microstructure of Continuous TiO₂ Fibers. *J Nanomater* 2012:1–7

Submit your manuscript to a SpringerOpen® journal and benefit from:

- Convenient online submission
- Rigorous peer review
- Open access: articles freely available online
- High visibility within the field
- Retaining the copyright to your article

Submit your next manuscript at ► springeropen.com